Article

Not peer-reviewed version

Seasonal Upwelling Shapes Coral Reef Community Structure and Photophysiology on the Pacific Coast of Costa Rica

Dar Golomb [†], Kayla M. Cayemitte [†], Grace K. Saba, Lori M. Garzio, Maxim Gorbunov, Clinton Haldeman, Juan José Alvarado, Tali Mass, Fiorella Prada [*]

Posted Date: 22 May 2026

doi: 10.20944/preprints202605.1556.v1

Keywords: coral reefs; coral photophysiology; benthic community composition; seasonal upwelling; Eastern Tropical Pacific; thermal refugia

 doi:10.20944/preprints202605.1556.v1

Article

Seasonal Upwelling Shapes Coral Reef Community Structure and Photophysiology on the Pacific Coast of Costa Rica

Dar Golomb [1,†], Kayla M. Cayemitte [2,†], Grace K. Saba [2], Lori M. Garzio [2], Maxim Gorbunov [2], Clinton Haldeman [2], Juan José Alvarado [3,4,5], Tali Mass [1] and Fiorella Prada [2,*]

[1] Department of Marine Biology, Leon H, Charney School of Marine Sciences, University of Haifa, Haifa, Israel

[2] Department of Marine and Coastal Sciences, Rutgers, The State University of New Jersey, New Brunswick, USA

[3] Escuela de Biología, Universidad de Costa Rica, San José, Costa Rica

[4] Centro de Investigación en Biodiversidad y Ecología Tropical (CIBET), Universidad de Costa Rica, San José, Costa Rica

[5] Centro de Investigación en Ciencias del Mar y Limnología (CIMAR), Universidad de Costa Rica, San José, Costa Rica

* Correspondence: prada@marine.rutgers.edu

† These authors contributed equally to this work.

Abstract

Reef-building corals form the calcium-carbonate frameworks that underpin tropical coral reefs, yet global coral cover has declined by ~50% in recent decades, due to marine heatwaves and other stressors. Identifying refugia environments, such as upwelling systems, that buffer stress, promote recovery, and enhance resilience by promoting physiological plasticity that supports thermotolerance is therefore critical. Here, we compared benthic community composition, coral percent cover, and photophysiology between an upwelling location in the Gulf of Papagayo and a non-upwelling location in Sámara on the Pacific coast of Costa Rica. Waters in Papagayo were cooler, more acidic, and richer in chlorophyll a. Reefs at this location exhibited higher crustose coralline algae, higher sea urchin cover, and lower macroalgae cover, compared to Sámara. Papagayo also showed higher stony coral cover, driven by Pocillopora spp., while Sámara was dominated by massive, heat-tolerant Porites spp.. When significant, photophysiological measurements showed 9.7 - 44.5% higher photosynthetic efficiency (F_v'/F_m') in Papagayo corals and 19.94 - 42.75 % higher maximum photosynthetic rates (P_{max}) in Sámara corals. These results highlight how contrasting environmental regimes within a relatively small geographic area can shape distinct coral community compositions and photophysiological strategies, with implications for identifying areas of reef persistence or refugia.

Keywords: coral reefs; coral photophysiology; benthic community composition; seasonal upwelling; Eastern Tropical Pacific; thermal refugia

1. Introduction

Tropical coral reefs are among the most biologically diverse and economically valuable ecosystems on Earth, yet they are increasingly threatened by climate-driven stressors, particularly ocean warming and ocean acidification [1–3]. The persistence and ecological success of coral reefs depend on the intracellular symbiosis between corals and dinoflagellates [4]. However, environmental stress can destabilize this partnership, resulting in the loss of photosymbionts in a process known as coral bleaching [5]. Elevated sea surface temperatures have driven recurrent mass

 doi:10.20944/preprints202605.1556.v1

bleaching events worldwide, leading to widespread mortality, structural degradation, and loss of ecosystem function [2,6]. Concurrently, rising atmospheric CO_2 has altered seawater carbonate chemistry, reducing pH and aragonite saturation state (Ω_{arag}), which can impair coral calcification and skeletal integrity [7,8]. Together, these stressors pose a substantial threat to reef persistence over the coming decades.

Despite these global trends, coral reef responses to climate change vary markedly across space, indicating that local environmental conditions can strongly shape coral vulnerability and resilience [9,10]. This spatial variability has driven growing interest in identifying natural refugia, that is, locations where physical or biological processes mitigate exposure to extreme thermal stress or enhance recovery potential [11,12]. Among these, coastal upwelling systems have emerged as candidate refugia due to their capacity to deliver cooler, nutrient-rich waters to shallow reef environments, thereby buffering corals from acute thermal extremes [1,13]. However, upwelling also brings CO_2-rich, lower-pH waters, raising important questions about whether thermal benefits outweigh the potential costs of chronic or episodic acidification [14,15].

The Pacific coast of Costa Rica provides a valuable natural laboratory for examining these dynamics. Reefs in this region experience pronounced seasonal and interannual variability driven by wind-forced upwelling and El Niño–Southern Oscillation (ENSO). The Gulf of Papagayo, located along the Pacific coast of Costa Rica, is one of the most intense and persistent upwelling centers in the Eastern Tropical Pacific (ETP), experiencing seasonal upwelling from December through April [16–18]. In contrast, nearby low upwelling regions are characterized by warmer, more thermally stable conditions and comparatively benign carbonate chemistry [19]. Few studies have considered this proximal spatial juxtaposition, which offers a powerful opportunity to disentangle the ecological and physiological consequences of upwelling exposure for coral reef communities under contemporary climate conditions. While direct studies of coral refugia in Costa Rican upwelling zones are lacking, research from the Pacific coast of Panamá demonstrates that upwelling can buffer reefs from thermal stress [13,20]. Recent work further suggests that corals exposed to seasonal upwelling endure more stressful baseline conditions, potentially contributing to elevated thermal thresholds, as inferred from host protein profiles [21].

Reef health and functioning emerge from the combined influence of reef structure, benthic cover, and biological diversity [22]. Structural complexity, generated by the three-dimensional framework of reef-building corals and other calcifying organisms, shapes habitat availability and ecological interactions, while metrics such as rugosity quantify this physical template [22,23]. At the same time, benthic cover and species richness provide complementary information on the biological state of reefs, reflecting patterns of dominance, functional roles, and demographic processes. Changes in coral cover, the relative abundance of benthic groups, and the identity and number of coral taxa can each signal shifts in reef condition, even when other metrics remain relatively stable [24–26]. Beyond structural and compositional metrics, coral photophysiology, typically assessed through chlorophyll fluorescence parameters such as the maximum quantum yield of photosystem II (F_v/F_m), provides a sensitive, sub-lethal indicator of the functional status of the coral–Symbiodiniaceae association, often detecting stress responses well before visible bleaching or mortality occur [27,28], Considered together, reef structural complexity, benthic cover, species composition, and coral photophysiology offer an integrated framework for assessing reef health and resilience, capturing both the physical foundation of reefs and the ecological and physiological processes that sustain them under environmental change.

Here, we investigated environmental variability, reef rugosity, benthic community composition, and coral photophysiological performance across upwelling-influenced reefs on the Pacific coast of Costa Rica, specifically in the strong upwelling location of the Gulf of Papagayo and a nearby weak upwelling location at Sámara. By integrating physical, chemical, ecological, and biological data, this study evaluates the potential for upwelling systems to function as thermal refugia for coral reefs.

2. Materials and Methods

 doi:10.20944/preprints202605.1556.v1

2.1. Study Location and Data Collection

The study was conducted at two locations along the Pacific coast of Costa Rica that experience contrasting seasonal upwelling regimes (Figure 1a). The Gulf of Papagayo (10.608739N 85.703523W) (Figure 1b) is influenced by frequent and strong upwelling, while Sámara Bay (9.864684N 85.51266W) is characterized by low upwelling conditions (Figure 1c). Strong wind jets that originate from the intensification of the trade winds and the southwardly intrusion of cold air masses during boreal winter, funnel through lowland gaps in Central America, resulting in strong offshore winds and subsequent upwelling [29] enhancing primary productivity and supporting diverse marine life. In comparison, Sámara Bay experiences weak upwelling, resulting in more stable and warmer seawater conditions throughout the year. Environmental and biological/ecological data were collected between 1-8 February 2025 and 13-22 February 2026 from 6 sites within the Gulf of Papagayo, from depths of 7.8- 10.8 m, and 4 sites within Sámara Bay from depths of 2.5-9.5 m. Fieldwork for this research was conducted under the research permit No. ACT-OR-DR-111-2024 issued by the Sistema Nacional de Áreas de Conservación (SINAC), Ministry of the Environment, Costa Rica.

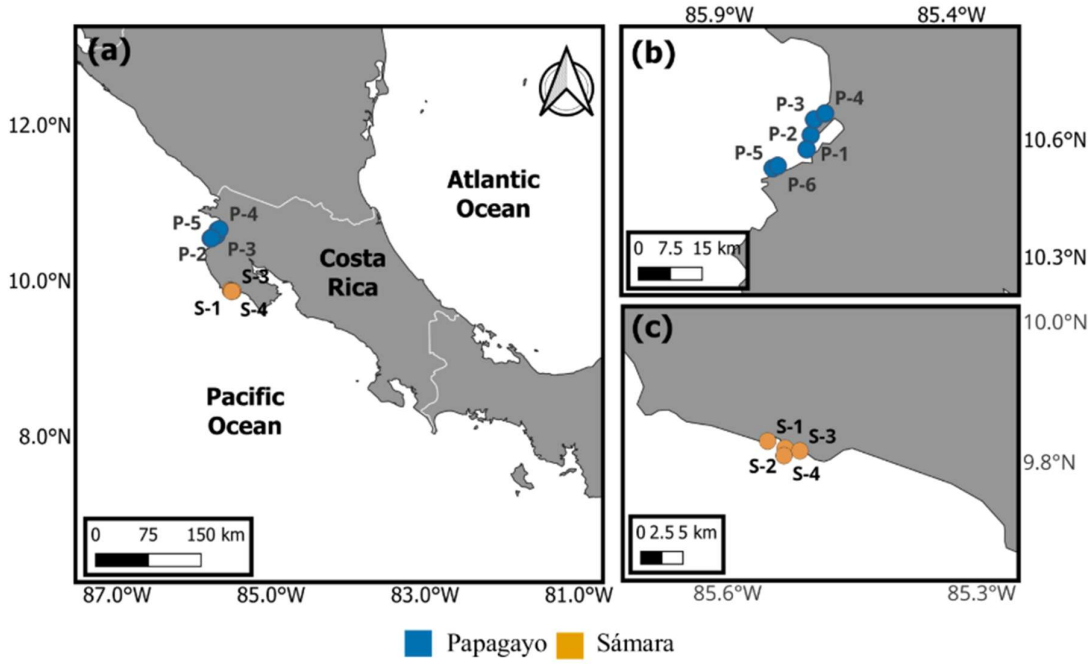

Figure 1. (a) Map of the two locations along the Pacific coast of Costa Rica, namely **(b)** Gulf of Papagayo, Guanacaste (10.6087N 85.7035W), and **(c)** Sámara Bay (9.8647N 85.5127W).

2.2. Environmental Conditions

Vertical profiles of temperature (°C), salinity (PSU), and chlorophyll-a (µg/L) were measured on board the vessel using a cage Sea-Bird SBE-19 Conductivity Temperature and Depth Sensor (CTD) [CTD; Sea-Bird Scientific, Bellevue, WA, USA]. Vertical profiles of pH were also measured by hand-lowering a YSI ProDSS Multiparameter Water Quality Meter [YSI Inc., Yellow Springs, OH, USA]. Discrete seawater samples for carbonate chemistry and dissolved inorganic nutrient analyses were collected by SCUBA using a 5-L Niskin bottle that was filled and closed in subsurface waters just above the coral communities. Three, 300 ml cleaned and combusted glass Biochemical Oxygen Demand (BOD) bottles were filled at each site, one for Dissolved Inorganic Carbon concentration (DIC) and Total Alkalinity (TA), and two for replicate pH measurements. Bottles were fully rinsed twice with seawater while tapping on the side of the bottle to eliminate any air bubbles before filling and capping the sample. Samples were then preserved with 0.02% $HgCl_2$, sealed, and kept on ice on the boat and then stored at 4 °C on land. All but one of Sámara's set of discrete carbonate chemistry

 doi:10.20944/preprints202605.1556.v1

samples were largely lost, while six discrete seawater samples were obtained from Papagayo. Remaining samples were analyzed for pH and TA/DIC at the University of New Hampshire (USA). pHT (pH on the Total Scale) was measured at 25 °C with purified meta-cresol purple [30] using 10 cm pathlength cylindrical glass cells and an Agilent Technologies Cary 8454 UV-Vis spectrometer [21]. DIC was measured using an Apollo SciTech AS-C2 [Apollo SciTech, Newark, DE, USA] automated analyzer. Certified seawater reference materials were used to determine DIC concentration by preparing a calibration curve covering the range of DIC from 200 to 2000 μmol kg^{-1} [32]. TA was determined utilizing titrations performed by a custom-built titration apparatus, following the approach of Standard Operating Procedure 3b [33]. Additional carbonate system parameters, including aragonite saturation state (Ω_{arag}), calcite saturation state (Ω_{calc}), $_pCO2$, HCO^{3-}, and CO_3^{2-} were calculated using PyCO2SYS [34] with pressure, temperature, salinity, TA, and DIC as the inputs [35].

Subsurface seawater from the 5-L Niskin bottle was also used to collect dissolved inorganic nutrient samples at each location as follows: three 50 mL replicates were collected and filtered through 0.2 μm sterile SFCA membrane syringe filters [Corning, Corning, NY, USA] using sterile B-D 60 mL syringes for Silicate (SiO2) content, and three 50 mL aliquots were collected for nitrate and phosphate (NO3/PO4). Samples were stored at -20 °C until processing. All labware was acid-washed, and samples were thawed to 4°C for processing. Calibration curves were generated using certified reference standards (KANSO Technos), and all samples were analyzed in triplicate with quality controls and blanks included in each run. Nutrient concentrations were determined using an AQ400 Discrete Analyzer (Seal Analytical) following standard colorimetric methods: nitrate (Method SEA-122-C Rev. 1), phosphate (Method SEA-156-C Rev. 1), and silicate (Method SEA-124-C Rev. 1).

2.3. Benthic Rugosity

To evaluate the structural complexity of the reef between locations, three-dimensional photogrammetric models of reef rugosity were generated using 5 × 5 m plots at each site. Images were collected by SCUBA diving with a GoPro Hero 12 in video mode (5.3K, 25 fps, wide-angle setting) with Bigblue Tech Dive Lights [36]. In each plot (6 in Sámara and 6 in Papagayo), targets were set. In order to ensure ~85% overlap between frames, videos were captured following a lawnmower pattern 1–2 m above the plot at a slow pace (~0.3–0.4 m/s), minimizing gaps in the resulting 3D reconstructions. Between 1,800 and 2,200 frames were extracted from each of the videos and processed in Agisoft Metashape Professional (version 2.2.1) to create digital elevation models (DEMs). The standard photogrammetric workflow was applied: image alignment, dense point cloud generation, and model scaling based on known reference marker dimensions [37,38]. Rugosity was calculated from the digital elevation model (DEM; .tif). The DEM was imported into R (v4.3.1) using the 'rast' function in the terra package, and terrain slope (radians) was derived with 'terrain'. For each rast cell, 3D surface area was computed as the cell planar area divided by the cosine of slope, and rugosity was expressed as the ratio of 3D surface area to 2D planar area (i.e., the product of cell resolutions) [39]. Because the rast contained a large number of cells, we randomly subsampled up to 1,000,000 rugosity values for statistical analyses using 'sample', ensuring a representative dataset while reducing computational demands.

2.4. Benthic Coverage

To quantify benthic cover, photo-quadrat surveys were conducted along randomly selected 30 m transects. Images were collected approximately every 2 m using a 0.5 m2 PVC quadrat frame (n = 15 quadrats per transect, 6 transects per site, 4 sites in Sámara and 6 sites in Papagayo). A Canon G7X Mark III camera in a Nauticam housing, fitted with a Fantasea Line UWL-09 67 mm wide-angle lens and illuminated with two Sea&Sea YS-D3 strobes, was mounted to the quadrat frame at a fixed height of 0.5 m above the reef to standardize image scale and lighting across samples/images [40]. Images were analyzed in CoralNet by annotating 25 randomly distributed points per quadrat. Points were manually classified to estimate the percent cover of 8 functional groups, including stony corals, soft

 doi:10.20944/preprints202605.1556.v1

corals, macroalgae, crustose coralline algae (CCA), sea urchins, filter feeders, and other benthic coverage. [35].

2.5. Photophysiology

In situ photophysiological measurements were taken at each location on *Pocillopora* spp., *Porites* spp., *Pavona* spp., and *Psammocora stellata* using a diver-operated Fluorescence Induction and Relaxation (FIRe) system [28], following protocols outlined by [28,41–43]. The Diving FIRe is programmed to conduct measurements in dark (when the sample is shaded, even during the daytime) and under saturating ambient light. The dark measurements provide information about characteristics that control the photosynthetic performance under low light (i.e., the initial slope of the photosynthesis-versus-irradiance curve), while measurements under saturating light yield the maximum photosynthetic rates (P_{max}).

For each of these sampling routines, the FIRe protocol comprises two distinct phases. In the first phase, a brief but intense 100-millisecond single-turnover flash is applied to saturate Photosystem II (PSII) within a single turnover. This step allows for the determination of key photosynthetic parameters, including the maximum quantum yield of PSII photochemistry (F_v'/F_m'), the functional absorption cross-section of PSII (Sigma: σPSII, in Å²), and the connectivity parameter (ϱ), which determines the probability of excitation energy transfer between adjacent PSII units (dimensionless) [28]. When the measurements are conducted on corals adapted to low or medium in situ irradiance, as on corals in turbid waters in the Papagayo, the measured F_v'/F_m', yields are very close to the dark-adapted values F_v/F_m, The second phase employs weak modulated light over a 200-millisecond period to capture the relaxation kinetics of fluorescence, which reflects the reoxidation kinetics of QA^- used to derived the time constant tau (τ), for electron transport on the acceptor side of PSII. To measure the maximum photosynthetic rate (P_{max}), the FIRe protocol is executed under saturating ambient light, which is automatically adjusted to an optimal level by the instrument computer, depending on the sample's photosynthetic properties [28]. The absolute maximum rate (P_{max}, in units of electrons s-1 per PSII) is calculated from the kinetic analysis of the fluorescence relaxation [28]. This kinetic analysis implemented in the FIRe instrument allows for P_{max} measurements in absolute units, so that numbers are not affected by highly variable pigment densities (i.e., "pigment packaging" effect); in turn, the values of P_{max} can be accurately compared between different samples. Thus, measured P_{max} reflects the so-called photosynthetic turnover rate, which is a characteristic of the overall rate of energy conversion efficiency from PSII to the carbon fixation cycle [44]

To account for intra-colony variability due to differences in ambient light exposure, five measurements are taken across different regions of each coral. Shaded areas, acclimated to low light, provide more accurate assessments of dark-adapted parameters (e.g., F_v'/F_m': photosynthetic efficiency), while sun-exposed regions of the coral conies offer accurate measurements of P_{max} and the photosynthetic turnover rate.

2.6. Statistics

All datasets were tested for normality and homogeneity of variances by applying the Shapiro–Wilk test ($n \leq 50$) or Kolmogorov–Smirnov test ($n > 50$), together with Levene's test for equality of variances [45–47]. When assumptions for parametric statistics were met, data between Sámara and Papagayo were compared using the parametric Student's t-test (only for photophysiology data for Sigma and connectivity parameter for *Pavona* spp.). When assumptions were not met, a non-parametric Mann–Whitney U test [48] was used for temperature, pH, salinity, chlorophyll-a, nitrate, phosphate, silicate, F_v'/F_m', F_m, P_{max}, τ, σPSII, and ϱ for all other species were non-parametric in Python 3.11 using the SciPy statistical package [49]. Rugosity between sites was compared using Welch's t-test, whereas benthic functional groups and cover of individual coral taxa were compared using the Mann-Whitney Test in R (R Core Team, 2024) using packages including tidyverse [50–52] rstatix [53], and ggpubr [53].

 doi:10.20944/preprints202605.1556.v1

3. Results

3.1. Environmental Conditions

Papagayo showed significantly lower temperature and pH and higher salinity and chlorophyll-a concentration compared to Sámara (Mann-Whitney test, $p < 0.001$, Figure 2, Table S1). While phosphate and nitrate were not different between locations, silicate was significantly lower in Papagayo compared to Sámara (Mann-Whitney, $p < 0.001$; Figure 2, Table S1). All but one of Sámara's set of discrete carbonate chemistry samples were largely lost, and although discrete data were obtained from six sites in Papagayo, statistical comparisons between locations were not possible. Therefore, we report here only qualitative trends. Seawater pH was significantly lower in Papagayo compared to Sámara, and carbonate ion (CO_3^{2-}), aragonite saturation state (Ω_{arag}), and calcite saturation state (Ω_{calc}) showed comparable trends between locations, whereas TA, DIC, *p*CO2, and bicarbonate (HCO^{3-}) showed higher values in Papagayo (Table S1).

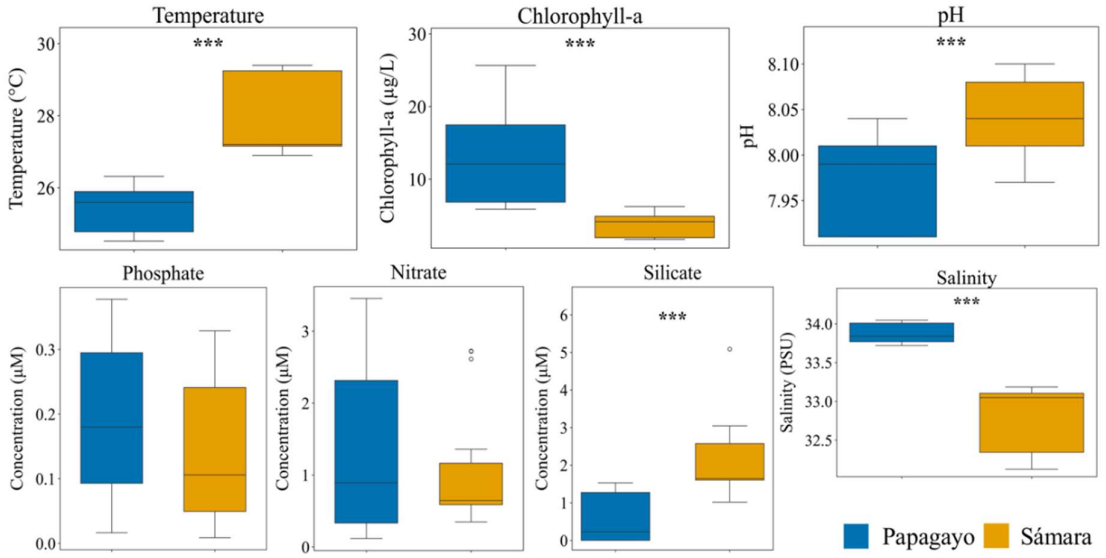

Figure 2. Temperature (°C), Salinity (PSU), Chlorophyll-a (µg/L), pH, Nitrate (µM), Phosphate (µM), and Silicate (µM) in Sámara and Papagayo. The boxes limit the 25th and 75th percentiles, and the line within the boxes marks the medians. Whisker length is equal to 1.5×interquartile range (IQR). Circles represent outliers. *** $p < 0.001$.

3.2. Benthic Rugosity

Reef structural complexity, quantified as rugosity, did not differ significantly between Papagayo and Sámara (Welch t-test, $p < 0.05$, Figure 3). Mean rugosity was higher at Papagayo (mean = 2.23) compared to Sámara (mean = 1.78). Although this difference did not reach conventional statistical significance, the effect size was large (Cohen's d = 1.29), indicating substantial separation between sites. Variability in rugosity was greater at Papagayo, as reflected by a wider interquartile range and greater dispersion of observations, whereas values at Sámara were more tightly clustered. Overall, rugosity exhibited a consistent directional trend toward higher structural complexity at Papagayo, suggesting a potential biologically meaningful difference between sites that may not have reached statistical significance due to limited sample size.

 doi:10.20944/preprints202605.1556.v1

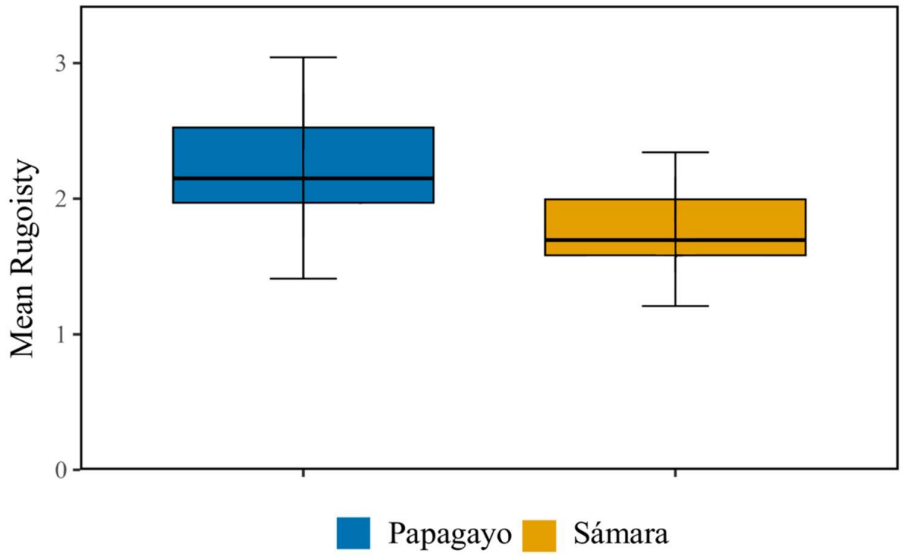

Figure 3. Reef rugosity at Papagayo and Sámara. The boxes limit the 25th and 75th percentiles, and the line within the boxes marks the medians. Whisker length is equal to 1.5×interquartile range (IQR). N = 6 at each location.

3.3. Benthic Cover

Benthic community structure differed between Papagayo and Sámara in a taxon- and functional group–specific manner. Stony coral cover was significantly higher in Papagayo compared to Sámara (Mann-Whitney Test, $p < 0.001$, Figure 4a, Table S3). Crustose coralline algae (CCA) exhibited significantly higher cover at Papagayo (Mann-Whitney Test, $p < 0.001$, Figure 4a, Table S3), while macroalgae were significantly more abundant at Sámara (Mann-Whitney Test, $p < 0.001$, Figure 4a, Table S3). Sea urchin cover was also significantly higher at Papagayo (Mann-Whitney Test, $p < 0.001$, Figure 4a, Table S3), while soft corals were significantly higher in Sámara (Mann-Whitney Test, $p < 0.05$, Figure 4a, Table S3). No significant differences were detected in filter feeders and other (i.e., gravel, sand, dead coral, rock, unknown) cover between locations (Mann-Whitney Test, $p < 0.05$, Figure 4a, Table S3). Analyses at finer taxonomic resolution revealed significant differences among individual coral taxa. Cover of *Pavona* spp. and *Pocillopora* spp. was significantly higher at Papagayo (Mann-Whitney Test, $p < 0.001$, Figure 4b, Table S4), whereas *Psammocora stellata* and *Porites* spp. exhibited higher cover at Sámara (Mann-Whitney Test, $p < 0.001$, Figure 4b, Table S4).

 doi:10.20944/preprints202605.1556.v1

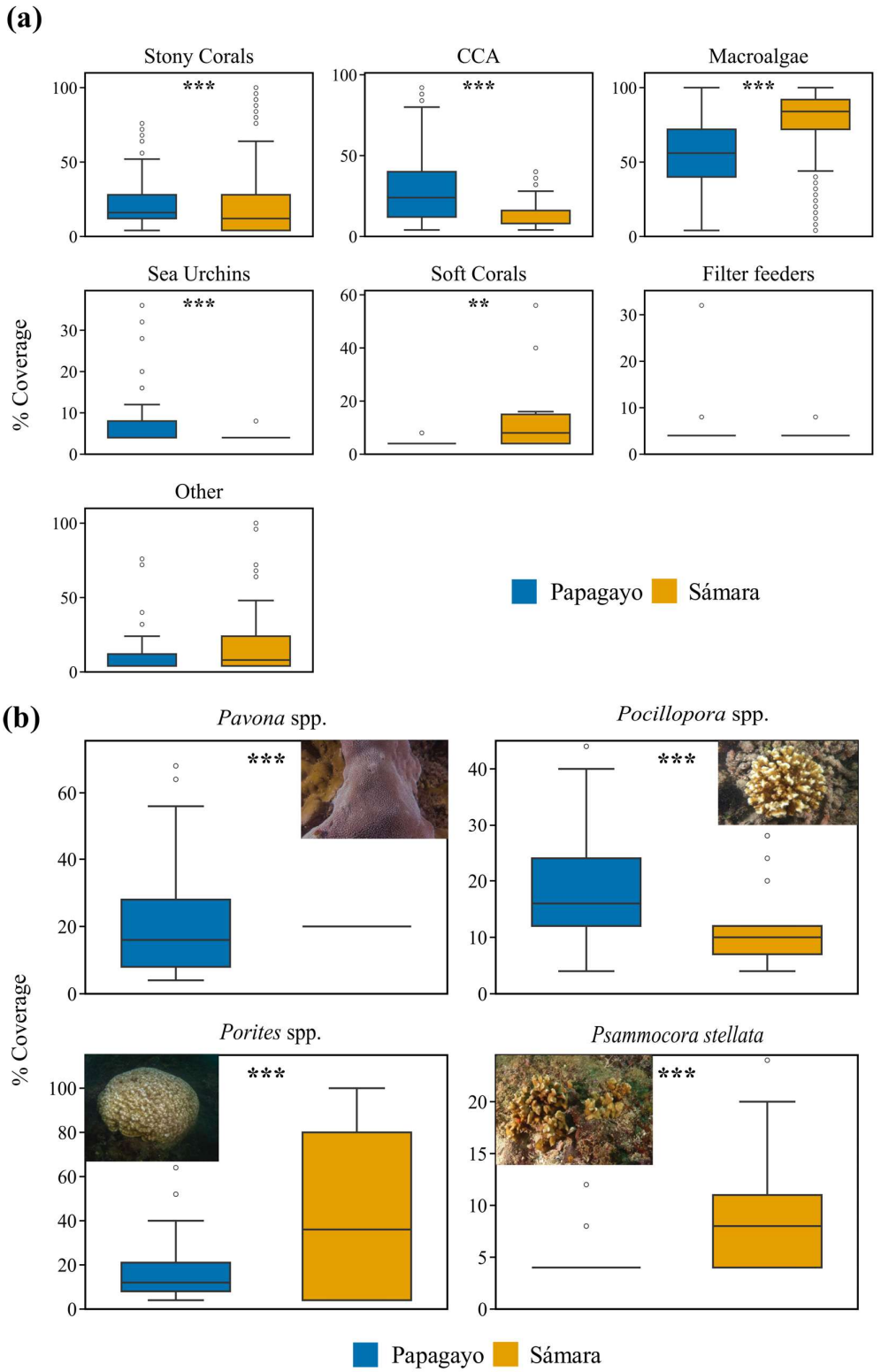

Figure 4. Comparison of benthic cover (%) between Papagayo and Sámara across functional groups and coral taxa. **(a)** Benthic functional groups, including crustose coralline algae (CCA), stony coral, filter feeders, macroalgae, sea urchins, soft corals, and other (i.e., gravel, sand, dead coral, rock, unknown). **(b)** Cover of individual coral taxa, including *Pavona* spp., *Pocillopora* spp., *Porites* spp., and *Psammocora stellata*. The boxes limit the 25th and 75th percentiles, and the line within the boxes marks the medians. Whisker length is equal to 1.5×interquartile range (IQR). Asterisks denote significant differences between sites based on the Mann-Whitney Test, *** $p < 0.001$, ** $p < 0.01$, * $p < 0.05$. NS indicated non-significant differences.

 doi:10.20944/preprints202605.1556.v1

3.4. Photophysiology

Photophysiology data were grouped by depth (shallow < 8 m, deep > 8 m) at both locations to account for possible light-driven effects. At shallow depths, F_v'/F_m' values were significantly higher in Papagayo than in Sámara for *Pocillopora* spp., *Porites* spp., and *Pavona* spp. (Mann-Whitney, $p < 0.05$, Figure 5a; Table S2). At the deeper depths, F_v'/F_m' values were significantly higher in Papagayo than in Sámara for *Porites* spp. and *Pavona* spp. (Mann-Whitney, $p < 0.001$, Figure 5a, Table S2). There were no significant differences between locations for F_v'/F_m' in *Psammocora stellata*. At shallow depths, Fm values were significantly lower in Papagayo than in Sámara for *Porites* spp. and *Psammocora stellata* (Mann-Whitney, shallow $p < 0.001$, Figure 5b, Table S2). At deeper depths, Fm values were significantly lower in Papagayo than in Sámara for *Pavona* spp. and significantly higher in Papagayo than in Sámara for *Porites* spp. (Mann-Whitney, deep $p < 0.001$, Figure 5b, Table S2). There were no significant differences between locations for F_m in *Pocillopora* spp.. At shallow depths, P_{max} values were significantly lower in Papagayo than in Sámara for *Pocillopora* spp., *Psammocora stellata* (Mann-Whitney, shallow $p < 0.001$, Figure 5c, Table S2), *Porites* spp., and *Pavona* spp. (Mann-Whitney, shallow $p < 0.01$, Figure 5c, Table S2). At deeper depths. P_{max} values were significantly lower in Papagayo than in Sámara for *Porites* spp. (Mann-Whitney, deep $p < 0.001$, Figure 5c, Table S2) and *Pavona* spp. (Mann-Whitney, shallow $p < 0.01$, Figure 5c, Table S2). All other photophysiological parameters, including τ, σPSII, and ϱ showed no significant differences (Figure S1). Overall, corals in Papagayo exhibited higher photochemical efficiency (F_v'/F_m')but lower maximum photosynthetic capacity (P_{max}) compared to Sámara across species.

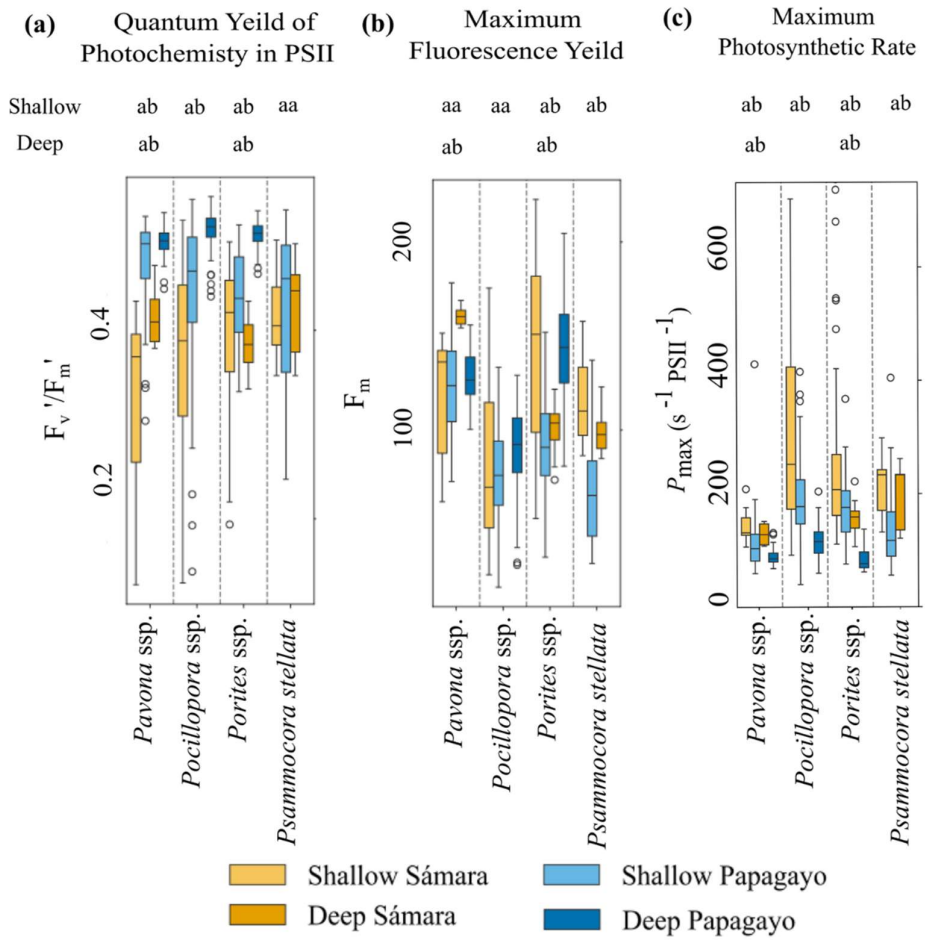

Figure 5. Photophysiological data for coral species *Pavona* ssp., *Pocillopora* spp., *Porites* spp., and *Psammocora stellata* between shallow (< 8 m) and deep (> 8m) sites in Papagayo and Sámara. a) F_v'/F_m' is the photosynthetic

 doi:10.20944/preprints202605.1556.v1

efficiency of photosystem II (PSII). b) Fm is the maximum fluorescence yield. c) P_{max} is the Maximum Electron Transport Rate. The boxes limit the 25th and 75th percentiles, and the line within the boxes marks the medians. Whisker length is equal to 1.5×interquartile range (IQR). "aa" indicates no significant difference, and "ab" indicates significant differences between groups in either shallow or deep categories.

4. Discussion

This study examined how environmental conditions, reef structural complexity, benthic assemblages, and coral photophysiology varied between strong upwelling-influenced reefs in the Gulf of Papagayo and the weak upwelling reefs in Sámara. Average temperatures, salinity, and pH values (Figure 2, Table S1) in Papagayo are in agreement with data collected in a recent study in the same area during the upwelling season [54]. Although statistical comparisons were not possible for carbonate chemistry parameters due to limited sampling at Sámara, DIC, TA, pCO_2, HCO^{3-}, CO_3^{2-}, Ω_{arag}, and Ω_{calc} values in Papagayo followed those of upwelled waters [54]. For instance, the onset of upwelling in the Gulf of Papagayo can cause drops in pH from 8.04 to 7.86 [54] and declines in temperature by 10 °C within hours [29,56,512], down to 17 °C in severe upwelling events [52]. Sámara's location is close enough to share regional conditions with Papagayo; however, it is sufficiently distant to reduce direct upwelling influence, resulting in a 10% higher observed average temperature, ~4% lower average salinity, and ~1% higher average pH when compared to Papagayo. While physical and chemical data for Southern Guanacaste are limited, reported average temperature and salinity values from Sámara during the non-upwelling season [57] are consistent with our observations.

The Gulf of Papagayo exhibits strong seasonal variability in nutrient concentrations, with elevated levels typically occurring during the dry season due to upwelling [58,59]. While our study showed that nitrate and phosphate were not significantly different between locations, they do trend higher in the Gulf of Papagayo compared to Sámara. Notably, our values (0.191 ± 0.127 μM PO_4^{3-}, 1.309 ± 1.192 μM NO_3^-) are comparably low to what we would expect in a high upwelling scenario (Figure 2, Table S1) where previous work shows that phosphate, and nitrate concentrations can increase 3–15 fold during upwelling events, reaching maxima of 1.3 μmol PO_4^{3-} L^{-1}, and 9.7 μmol NO_3^- L^{-1} [59] . Upwelling-driven nutrient inputs in this region are known to stimulate phytoplankton blooms, often reflected by increases in chlorophyll a concentrations up to 1.20 ± 0.50 μg L^{-1} during upwelling events [59]. The higher chlorophyll a concentrations observed in our study (12.5 ± 5.40 μg L^{-1}) suggest that upwelling indeed stimulated a substantial phytoplankton bloom. This bloom development likely resulted in rapid biological uptake and subsequent drawdown of dissolved nutrients, which may explain the relatively low nutrient concentrations at the time of our observations. In agreement with this observation, silicate, which is a limiting nutrient required by diatoms to construct their siliceous frustules [60], was significantly lower in Papagayo (0.538 ± 0.623 μM) compared to Sámara (2.140 ± 1.020 μM), likely reflecting silicate drawdown during commonly occurring diatom-dominated phytoplankton blooms in the region [61]. Overall, our analysis indicates that despite their close geographic proximity, these sites experience distinct environmental conditions consistent with the different intensities of upwelling that shape the physicochemical regimes under which corals grow.

Reef rugosity, known as the variation of amplitude in the height of a surface, is a proxy for structural complexity [62,63]. While not significant, overall rugosity values trended higher in Papagayo compared to Sámara, suggesting that rugosity may support more coral reef accretion [64]. Our findings are consistent with model predictions that indicate higher reef accretion potential in ETP upwelling zones (up to 5.5 mm yr^{-1}) compared to weak upwelling regions (0.3 mm yr^{-1}) [20], and support the idea that coral growth might be enhanced under upwelling conditions. Furthermore, as branching corals contribute more surface complexity than mound- or boulder-shaped corals [65], the greater abundance of *Pocillopora* spp. in Papagayo compared to Sámara, may explain the rugosity observed at this location. Structural complexity and benthic community composition are tightly

 doi:10.20944/preprints202605.1556.v1

coupled in coral reef environments: habitat heterogeneity promotes benthic persistence, while the composition of the benthos, in turn, shapes and maintains the physical structure of the reef [66].

Indeed, benthic cover differed across functional groups when comparing Sámara and Papagayo. The latter exhibited significantly higher stony coral, crustose coralline algae (CCA), and sea urchin coverage, along with lower macroalgal cover and soft coral coverage compared to Sámara. Macroalgae are well-established competitors of corals, capable of suppressing coral growth and reducing photosynthetic efficiency through direct interactions [67]. They also compete for benthic space [68], and once established, can inhibit coral recruitment and persistence, making recovery of coral-dominated states more difficult [69,70]. In the Gulf of Papagayo, seasonal upwelling and associated nutrient enrichment are typically expected to promote algal proliferation and influence benthic succession [71]. However, the lower macroalgal cover observed in Papagayo relative to Sámara suggests that additional ecological controls may be limiting macroalgal dominance. Sea urchins such as *Diadema mexicanum* have been documented to play a key role in structuring benthic communities in the ETP through grazing and bioerosion, with disturbances such as El Niño increasing macroalgal abundance and subsequently eliciting a regulatory response from urchin populations [72]. The higher abundance of sea urchins in Papagayo, therefore, suggests elevated herbivory pressure in this area. Additionally, the barren benthic conditions resulting from herbivory by sea urchins promote CCA-dominated substrates [73]. Notably, CCAs are early colonizers of newly available benthic substrates, particularly in areas subjected to intense herbivory, as their encrusting morphology and resistance to grazing allow them to rapidly establish and persist under these conditions [74,75]. CCAs are known to facilitate coral larval settlement by providing both chemical and microbial cues that induce attachment and metamorphosis [76,77]. This enhanced settlement success can increase coral recruitment rates of stony coral populations, which may in part explain the increasing trend in stony coral cover observed at the upwelling location.

When examining coral community cover, we observed species-specific differences between the two locations. For instance, *Pocillopora* spp., and *Pavona* spp. dominated in Papagayo, while Sámara showed a higher cover in *Psammocora stellata* and *Porites* spp.. Our findings align with other studies where *Pocillopora* spp. and *Pavona* spp. are known to dominate Northern regions of the Costa Rican Pacific coast [54,78,79] whereas *Porites* spp. and *Psammocora* spp. are the main reef-forming corals in the south [54,80,81]. As the most common coral genus in the ETP, *Pocillopora* spp. are highly flexible and able to persist across a wide range of environmental conditions [82]. At upwelling-influenced reefs around Gorgona Island (Colombia) *Pocillopora* spp. colonies experience environmental conditions similar to those observed in our study [83]. However, findings indicate reduced metabolic performance and calcification rates, alongside increased symbiont densities, suggesting that although these corals persist under upwelling conditions, they may be operating near their physiological limits. Despite exposure to substantial environmental variability in the Gulf of Papagayo, *Pocillopora* spp. and *Pavona* spp. have been reported to exhibit higher linear extension rates than conspecifics in non-upwelling regions, indicating a capacity for adaptation or acclimatization to cooler, acidified upwelled waters [84]. Indeed, the high nutrient input from upwelling may provide conditions for optimal growth, as reported growth rates from *Pocillopora* spp., *P. clavus*, and *P. stellata* were some of the highest documented across the ETP [85]. Similarly, a study on *P. stellata* and *P. profundacella* across upwelling and non-upwelling regions of the ETP found that reproductive activity in upwelling environments is more pronounced during warmer periods, whereas more thermally stable environments support protracted reproductive activity throughout the year [84]. Such variation in reproductive timing may represent an adaptive response, enabling persistence under variable environmental conditions.

Additionally, benthic coverage of *Porites* spp. increases toward the southern portion of the Costa Rican Pacific coast [81]. This spatial pattern is consistent with prior work showing that *Porites* spp. are well adapted to low salinity, reduced Ω_{arag}, and diminished light availability associated with terrigenous input during the rainy season that characterizes these southern regions [54,86]. *Porites* spp. are widely recognized as stress-tolerant corals with greater thermal resilience than branching

 doi:10.20944/preprints202605.1556.v1

genera such as *Pocillopora*, owing in part to their thick tissues [87], greater mass transfer rates [88] and elevated metabolism [89]. Field observations across the ETP initially support this: during the 1983 bleaching event, only ~14% of *Porites* lobata colonies were affected, compared to 70–88% of *Pocillopora* spp. [90]. However, subsequent bleaching events in the ETP have revealed a more nuanced picture. *Pocillopora* spp. have exhibited increasing heat resistance over time, likely driven by their capacity to host the thermotolerant symbiont *Durusdinium glynnii* [90], combined with high growth rates and asexual reproduction through fragmentation, which together confer a higher recovery capacity compared to other scleractinians [90]. In contrast, non-pocilloporid corals in the ETP, including P. lobata, have either remained highly susceptible to heat stress or shown only moderate tolerance that diminishes under increasingly extreme bleaching conditions [90]. This disparity may be linked to symbiont community composition: non-pocilloporid species in the ETP predominantly host *Cladocopium*, with thermotolerant genera such as *Durusdinium* detected only at background densities [90]. Additionally, work from American Samoa suggests that highly variable thermal environments may further reduce thermal tolerance in *Porites* relative to more stable ones [91]. Their skeletal properties appear to be sensitive to nutrient dynamics; elevated phosphate concentrations associated with upwelling have been shown to reduce skeletal density in *Porites* spp. in the Galápagos [92]. The reduced prevalence of *Porites* spp. in Papagayo may therefore reflect the challenges posed by the variable upwelling conditions at this site, where cooler thermal fluctuations, elevated nutrient concentrations, and the lack of symbiont-mediated thermal advantages available to *Pocillopora* may collectively limit the long-term reef-building capacity in this genus.

Beyond these community-level patterns, the photophysiological responses of the coral holobiont offer further insight into how species respond to the contrasting environmental regimes of Papagayo and Sámara. Photophysiological data collected in situ on the four investigated coral species provide insight into physiological adaptation mechanisms to upwelling vs. non-upwelling conditions. F_m, the maximum yields of chlorophyll-a fluorescence measured in a dark-adapted state [93], did not show a decrease in shallow corals compared to deeper corals, suggesting there are no confounding light effects when comparing corals between Papagayo and Sámara [94]. Therefore, differences in photochemical properties (F_v'/F_m' and P_{max}) between locations, as discussed below, are likely driven by other environmental factors [42]. Higher F_v'/F_m' values observed in Papagayo across multiple taxa show enhanced photochemical efficiency in this upwelling-influenced environment [27,43]. While interspecific comparisons in photophysiology are beyond the scope of this study, it is worth noting that F_v'/F_m' values in Papagayo trended slightly higher in *Pocillopora* spp. compared to *Porites* spp., a pattern that could reflect the association of *Pocillopora* spp. with the thermotolerant symbiont *Durusdinium glynnii* [90]. Enhanced photochemical efficiency in the upwelling location is also consistent with previous findings from the Southern Line Islands, where photophysiological responses were examined along a natural gradient in inorganic nutrients associated with upwelling [95]. Findings demonstrate that nutrient stress leads to a decrease in the quantum yield of photochemistry in Photosystem II (F_v/F_m) [28]. This mechanism may help explain the elevated F_v'/F_m' values observed in Papagayo, where exposure to higher dissolved inorganic nitrogen and phosphorus levels [96] could enhance the capacity of symbiotic algae to build and maintain functional photosystem complexes [82]. P_{max}, defined as the maximum rate of photosynthesis at saturating irradiance [98], reflects the photosynthetic turnover rate, i.e., the integrated performance of the photosynthetic apparatus, which is mechanistically influenced by the number of functional photosynthetic units and the efficiency of all steps of electron transport down to carbon fixation [99]. In this study, we found that the corals from Sámara exhibited higher Pmax values despite lower F_v'/F_m'. As P_{max} has been observed to increase across a gradient of temperatures across reefs and then sharply decline above a thermal optimum [100], our results indicate physiological acclimation to warm conditions in Sámara. The observed plasticity of P_{max} [98] suggests that targeted thermotolerance experiments are needed to further validate this interpretation [42,93].

 doi:10.20944/preprints202605.1556.v1

5. Conclusions

Overall, our results demonstrate that upwelling and non-upwelling reef environments in the Pacific coast of Costa Rica are not only distinct across physical, chemical, ecological, and physiological dimensions, but are structured by fundamentally different environmental pressures that shape coral persistence strategies. The cooler, more variable, and nutrient-enhanced conditions in upwelling regions such as the Gulf of Papagayo may promote physiological plasticity and enhance photochemical performance, potentially increasing coral tolerance to thermal stress, while more stable, warmer environments like Sámara favor persistent taxa. These patterns support the idea that upwelling systems could function as natural refugia during marine heatwaves, as has been suggested in other regions [13,101], by buffering extreme temperatures and sustaining coral populations that may contribute to regional recovery. However, the ecological benefits of these systems likely depend on minimizing additional local anthropogenic stressors, underscoring the importance of targeted conservation and management in upwelling-influenced reefs. Future work should directly test these hypotheses through controlled thermotolerance experiments, alongside gene expression and microbiome analyses, to better resolve the mechanistic basis of resilience and determine the extent to which these environments can support coral persistence under continued climate change.

Supplementary Materials: The following supporting information can be downloaded at the website of this paper posted on Preprints.org, Figure S1: Photophysiological data; Table S1: Physical Conditions; Table S2: Average photophysiological data for coral species; Table S3: Benthic Composition; Table S4: Coral Composition.

Author Contributions: Conceptualization, F.P.; methodology, D.G., K.C., G.S., C.H., T.M., and F.P.; software, D.G., K.C., G.S., L.G, M.G., T.M., and F.P.; validation, G.S., L.G., M.G., T.M., and F.P.; formal analysis, D.G., K.C., G.S., L.G. and F.P; investigation, D.G., K.C., G.S., T.M., F.P.; resources G.S., M.G., T.M., F.P.; data curation, D.G. and K.C.; writing—original draft preparation, D.G., K.C.; writing—review and editing, K.C., G.S., L.G, M.G., J.J.A., T.M., and F.P.; visualization, D.G., K.C.; supervision, T.M. and F.P.; project administration, F.P.; funding acquisition, T.M. and F.P. All authors have read and agreed to the published version of the manuscript.

Funding: Funding for this project was from the Rutgers Global Environmental Change Grant and from the University of Haifa Global Engagement Research Fund.

Data Availability Statement: All data needed to evaluate the conclusions in this paper are available in the paper, SI Materials, GitHub repository (DOI: 10.5281/zenodo.17097863); these data will be publicly released upon publication of this manuscript.

Acknowledgments: The research leading to these results has received funding from the Rutgers Global Environmental Change Grant and from the University of Haifa Global Engagement Research Fund. A team effort to produce this research was made possible by Proyecto Corales de Sámara and the Universidad de Costa Rica (UCR), which aided in underwater activities in the field. We are grateful to Will Biggs for nutrient sample preparation, and Lori Garzio and Nicole Waite for assistance with field equipment preparation.

Conflicts of Interest: The authors declare no conflicts of interest.

Abbreviations

The following abbreviations are used in this manuscript:

DIC	Dissolved Inorganic Carbon
TA	Total Alkalinity
Ω_{arag}	Aragonite saturation state
CCA	Crustose coralline algae

 doi:10.20944/preprints202605.1556.v1

References

1. Fox, M.D.; Guillaume-Castel, R.; Edwards, C.B.; Glanz, J.; Gove, J.M.; Green, J.A.M.; Juhlin, E.; Smith, J.E.; Williams, G.J. Ocean Currents Magnify Upwelling and Deliver Nutritional Subsidies to Reef-Building Corals during El Niño Heatwaves. Sci. Adv. 2023, 9, eadd5032, doi:10.1126/sciadv.add5032.
2. Hughes, T.P.; Kerry, J.T.; Baird, A.H.; Connolly, S.R.; Dietzel, A.; Eakin, C.M.; Heron, S.F.; Hoey, A.S.; Hoogenboom, M.O.; Liu, G.; et al. Global Warming Transforms Coral Reef Assemblages. Nature 2018, 556, 492–496, doi:10.1038/s41586-018-0041-2.
3. Hoegh-Guldberg, O.; Mumby, P.J.; Hooten, A.J.; Steneck, R.S.; Greenfield, P.; Gomez, E.; Harvell, C.D.; Sale, P.F.; Edwards, A.J.; Caldeira, K.; et al. Coral Reefs Under Rapid Climate Change and Ocean Acidification. Science 2007, 318, 1737–1742, doi:10.1126/science.1152509.
4. Davy, S.K.; Allemand, D.; Weis, V.M. Cell Biology of Cnidarian-Dinoflagellate Symbiosis. Microbiol Mol Biol Rev 2012, 76, 229–261, doi:10.1128/MMBR.05014-11.
5. Downs, C.A.; McDougall, K.E.; Woodley, C.M.; Fauth, J.E.; Richmond, R.H.; Kushmaro, A.; Gibb, S.W.; Loya, Y.; Ostrander, G.K.; Kramarsky-Winter, E. Heat-Stress and Light-Stress Induce Different Cellular Pathologies in the Symbiotic Dinoflagellate during Coral Bleaching. PLoS One 2013, 8, e77173, doi:10.1371/journal.pone.0077173.
6. Reimer, J.D.; Peixoto, R.S.; Davies, S.W.; Traylor-Knowles, N.; Short, M.L.; Cabral-Tena, R.A.; Burt, J.A.; Pessoa, I.; Banaszak, A.T.; Winters, R.S.; et al. The Fourth Global Coral Bleaching Event: Where Do We Go from Here? Coral Reefs 2024, 43, 1121–1125, doi:10.1007/s00338-024-02504-w.
7. Kwiatkowski, L.; Torres, O.; Bopp, L.; Aumont, O.; Chamberlain, M.; Christian, J.R.; Dunne, J.P.; Gehlen, M.; Ilyina, T.; John, J.G.; et al. Twenty-First Century Ocean Warming, Acidification, Deoxygenation, and Upper-Ocean Nutrient and Primary Production Decline from CMIP6 Model Projections. Biogeosciences 2020, 17, 3439–3470, doi:10.5194/bg-17-3439-2020.
8. Doney, S.C.; Fabry, V.J.; Feely, R.A.; Kleypas, J.A. Ocean Acidification: The Other CO2 Problem. Annu. Rev. Mar. Sci. 2009, 1, 169–192, doi:10.1146/annurev.marine.010908.163834.
9. Darling, E.S.; Côté, I.M. Seeking Resilience in Marine Ecosystems. Science 2018, 359, 986–987, doi:10.1126/science.aas9852.
10. McClanahan, T.R.; Maina, J.M.; Darling, E.S.; Guillaume, M.M.M.; Muthiga, N.A.; D'agata, S.; Leblond, J.; Arthur, R.; Jupiter, S.D.; Wilson, S.K.; et al. Large Geographic Variability in the Resistance of Corals to Thermal Stress. Global Ecol. Biogeogr. 2020, 29, 2229–2247, doi:10.1111/geb.13191.
11. Camp, E.F.; Schoepf, V.; Mumby, P.J.; Suggett, D.J. Editorial: The Future of Coral Reefs Subject to Rapid Climate Change: Lessons From Natural Extreme Environments. Front. Mar. Sci. 2018, 5, 433, doi:10.3389/fmars.2018.00433.
12. Van Hooidonk, R.; Maynard, J.; Tamelander, J.; Gove, J.; Ahmadia, G.; Raymundo, L.; Williams, G.; Heron, S.F.; Planes, S. Local-Scale Projections of Coral Reef Futures and Implications of the Paris Agreement. Sci Rep 2016, 6, 39666, doi:10.1038/srep39666.
13. Randall, C.J.; Toth, L.T.; Leichter, J.J.; Maté, J.L.; Aronson, R.B. Upwelling Buffers Climate Change Impacts on Coral Reefs of the Eastern Tropical Pacific. Ecology 2020, 101, e02918, doi:10.1002/ecy.2918.
14. Feely, R.A.; Sabine, C.L.; Hernandez-Ayon, J.M.; Ianson, D.; Hales, B. Evidence for Upwelling of Corrosive "Acidified" Water onto the Continental Shelf. Science 2008, 320, 1490–1492, doi:10.1126/science.1155676.
15. Kapsenberg, L.; Cyronak, T. Ocean Acidification Refugia in Variable Environments. Global Change Biology 2019, 25, 3201–3214, doi:10.1111/gcb.14730.
16. Sánchez-Noguera, C.; Stuhldreier, I.; Cortés, J.; Jiménez, C.; Morales, Á.; Wild, C.; Rixen, T. Natural Ocean Acidification at Papagayo Upwelling System (North Pacific Costa Rica): Implications for Reef Development. Biogeosciences 2018, 15, 2349–2360, doi:10.5194/bg-15-2349-2018.
17. Sun, C.-Y.; Stifler, C.A.; Chopdekar, R.V.; Schmidt, C.A.; Parida, G.; Schoeppler, V.; Fordyce, B.I.; Brau, J.H.; Mass, T.; Tambutté, S.; et al. From Particle Attachment to Space-Filling Coral Skeletons. Proc. Natl. Acad. Sci. U.S.A. 2020, 117, 30159–30170, doi:10.1073/pnas.2012025117.
18. Cambronero-Solano, S.; Tisseaux-Navarro, A.; Vargas-Hernández, J.-M.; Salazar-Ceciliano, J.-P.; Benavides-Morera, R.; Quesada-Ávila, I.; Brenes-Rodríguez, C. Hydrographic Variability in the Gulf of Papagayo, Costa Rica during 2017-2019. RBT 2021, 69, S74–S93, doi:10.15517/rbt.v69iSuppl.2.48308.

 doi:10.20944/preprints202605.1556.v1

19. Cortés, J.; Jiménez, C.E.; Fonseca, A.C.; Alvarado, J.J. Status and conservation of coral reefs in Costa Rica. Revista de Biología Tropical 2010, 58, 33–50.
20. Rodriguez-Ruano, V.; Toth, L.T.; Enochs, I.C.; Randall, C.J.; Aronson, R.B. Upwelling, Climate Change, and the Shifting Geography of Coral Reef Development. Sci Rep 2023, 13, 1770, doi:10.1038/s41598-023-28489-0.
21. Glynn, V.M.; De Barros Marangoni, L.F.; Guglielmetti, M.; Tapia, E.R.; Ali, V.; Quintero, H.; Rodriguez Guerra, E.C.; Yuval, M.; Kline, D.I.; Leray, M.; et al. The Role of Holobiont Composition and Environmental History in Thermotolerance of Tropical Eastern Pacific Corals. Current Biology 2025, 35, 3048-3063.e7, doi:10.1016/j.cub.2025.05.035.
22. Graham, N.A.J.; Nash, K.L. The Importance of Structural Complexity in Coral Reef Ecosystems. Coral Reefs 2013, 32, 315–326, doi:10.1007/s00338-012-0984-y.
23. Darling, E.S.; Graham, N.A.J.; Januchowski-Hartley, F.A.; Nash, K.L.; Pratchett, M.S.; Wilson, S.K. Relationships between Structural Complexity, Coral Traits, and Reef Fish Assemblages. Coral Reefs 2017, 36, 561–575, doi:10.1007/s00338-017-1539-z.
24. McClanahan, T.R.; Graham, N.A.J.; MacNeil, M.A.; Muthiga, N.A.; Cinner, J.E.; Bruggemann, J.H.; Wilson, S.K. Critical Thresholds and Tangible Targets for Ecosystem-Based Management of Coral Reef Fisheries. Proc. Natl. Acad. Sci. U.S.A. 2011, 108, 17230–17233, doi:10.1073/pnas.1106861108.
25. Darling, E.S.; Alvarez-Filip, L.; Oliver, T.A.; McClanahan, T.R.; Côté, I.M. Evaluating Life-history Strategies of Reef Corals from Species Traits. Ecology Letters 2012, 15, 1378–1386, doi:10.1111/j.1461-0248.2012.01861.x.
26. Brito-Millán, M.; Werner, B.T.; Sandin, S.A.; McNamara, D.E. Influence of Aggregation on Benthic Coral Reef Spatio-Temporal Dynamics. R. Soc. open sci. 2019, 6, 181703, doi:10.1098/rsos.181703.
27. Alfaro, E.J.; Cortés, J. Atmospheric Forcing of Cool Subsurface Water Events in Bahía Culebra, Gulf of Papagayo, Costa Rica. RBT 2015, 60, 173, doi:10.15517/rbt.v60i2.20001.
28. Liu, X.; Patsavas, M.C.; Byrne, R.H. Purification and Characterization of Meta-Cresol Purple for Spectrophotometric Seawater pH Measurements. Environ. Sci. Technol. 2011, 45, 4862–4868, doi:10.1021/es200665d.
29. Douglas, N.K.; Byrne, R.H. Achieving Accurate Spectrophotometric pH Measurements Using Unpurified Meta-Cresol Purple. Marine Chemistry 2017, 190, 66–72, doi:10.1016/j.marchem.2017.02.004.
30. Guide to Best Practices for Ocean CO2 Measurements; Dickson, A.G., Sabine, C.L., Christian, J.R., Bargeron, C.P., North Pacific Marine Science Organization, Eds.; PICES special publication; North Pacific Marine Science Organization: Sidney, BC, 2007; ISBN 978-1-897176-07-8.
31. Dickson, A.G.; Afghan, J.D.; Anderson, G.C. Reference Materials for Oceanic CO2 Analysis: A Method for the Certification of Total Alkalinity. Marine Chemistry 2003, 80, 185–197, doi:10.1016/S0304-4203(02)00133-0.
32. Humphreys, M.P.; Lewis, E.R.; Sharp, J.D.; Pierrot, D. PyCO2SYS v1.8: Marine Carbonate System Calculations in Python. Geoscientific Model Development 2022, 15, 15–43, doi:10.5194/gmd-15-15-2022.
33. Lewis, E.R.; Wallace, D. OCADS - Program Developed for CO2 System Calculations Available online: https://www.ncei.noaa.gov/access/ocean-carbon-acidification-data-system/oceans/CO2SYS/co2rprt.html (accessed on 5 November 2025).
34. Sauder, J.; Banc-Prandi, G.; Meibom, A.; Tuia, D. Scalable Semantic 3D Mapping of Coral Reefs with Deep Learning. Methods in Ecology and Evolution 2024, 15, 916–934, doi:10.1111/2041-210X.14307.
35. Cook, S. Standard Operating Procedures for the Use of Large-Area Imaging in Tropical Shallow Water Coral Reef Monitoring, Research and Restoration: Applications for Mission: Iconic Reefs Restoration in the Florida Keys National Marine Sanctuary. 2023, doi:10.25923/W8H9-4Z75.
36. Urbina-Barreto, I.; Chiroleu, F.; Pinel, R.; Fréchon, L.; Mahamadaly, V.; Elise, S.; Kulbicki, M.; Quod, J.-P.; Dutrieux, E.; Garnier, R.; et al. Quantifying the Shelter Capacity of Coral Reefs Using Photogrammetric 3D Modeling: From Colonies to Reefscapes. Ecological Indicators 2021, 121, 107151, doi:10.1016/j.ecolind.2020.107151.
37. Du Preez, C. A New Arc–Chord Ratio (ACR) Rugosity Index for Quantifying Three-Dimensional Landscape Structural Complexity. Landscape Ecol 2015, 30, 181–192, doi:10.1007/s10980-014-0118-8.

 doi:10.20944/preprints202605.1556.v1

38. Lechene, M.A.A.; Haberstroh, A.J.; Byrne, M.; Figueira, W.; Ferrari, R. Optimising Sampling Strategies in Coral Reefs Using Large-Area Mosaics. Remote Sensing 2019, 11, 2907, doi:10.3390/rs11242907.
39. Gorbunov, M.Y.; Falkowski, P.G. Using Chlorophyll Fluorescence Kinetics to Determine Photosynthesis in Aquatic Ecosystems. Limnology & Oceanography 2021, 66, 1–13, doi:10.1002/lno.11581.
40. Goodbody-Gringley, G.; Martinez, S.; Bellworthy, J.; Chequer, A.; Nativ, H.; Mass, T. Irradiance Driven Trophic Plasticity in the Coral Madracis Pharensis from the Eastern Mediterranean. Sci Rep 2024, 14, 3646, doi:10.1038/s41598-024-54217-3.
41. Carpenter, G.E.; Chequer, A.D.; Weber, S.; Mass, T.; Goodbody-Gringley, G. Light and Photoacclimatization Drive Distinct Differences between Shallow and Mesophotic Coral Communities. Ecosphere 2022, 13, e4200, doi:10.1002/ecs2.4200.
42. Gorbunov, M.Y.; Falkowski, P.G. Fluorescence Induction and Relaxation (FIRe) Technique and Instrumentation for Monitoring Photosynthetic Processes and Primary Production in Aquatic Ecosystems. In Proceedings of the Proc. 13th International Congress of Photosynthesis; Allen Press: Montreal, 2005; pp. 1029–1031.
43. Gorbunov, M.Y.; Falkowski, P.G. Using Chlorophyll Fluorescence to Determine the Fate of Photons Absorbed by Phytoplankton in the World's Oceans. Annu. Rev. Mar. Sci. 2022, 14, 213–238, doi:10.1146/annurev-marine-032621-122346.
44. Shapiro, S.S.; Wilk, M.B. An Analysis of Variance Test for Normality (Complete Samples). Biometrika 1965, 52, 591, doi:10.2307/2333709.
45. Massey, F.J. The Kolmogorov-Smirnov Test for Goodness of Fit. Journal of the American Statistical Association 1951, 46, 68–78, doi:10.1080/01621459.1951.10500769.
46. Levene, H. Robust Tests for Equality of Variances. Contributions to Probability and Statistics: Essays in Honor of Harold Hotelling. 1960, 278–292.
47. Mann, H.B.; Whitney, D.R. On a Test of Whether One of Two Random Variables Is Stochastically Larger than the Other. Ann. Math. Statist. 1947, 18, 50–60, doi:10.1214/aoms/1177730491.
48. Virtanen, P.; Gommers, R.; Oliphant, T.E.; Haberland, M.; Reddy, T.; Cournapeau, D.; Burovski, E.; Peterson, P.; Weckesser, W.; Bright, J.; et al. SciPy 1.0: Fundamental Algorithms for Scientific Computing in Python. Nat Methods 2020, 17, 261–272, doi:10.1038/s41592-019-0686-2.
49. D'Olivo, J.P.; McCulloch, M.T. Response of Coral Calcification and Calcifying Fluid Composition to Thermally Induced Bleaching Stress. Sci Rep 2017, 7, 2207, doi:10.1038/s41598-017-02306-x.
50. Spring, D.L.; Williams, G.J. Influence of Upwelling on Coral Reef Benthic Communities: A Systematic Review and Meta-Analysis. Proc. R. Soc. B. 2023, 290, 20230023, doi:10.1098/rspb.2023.0023.
51. Rixen, T.; Jiménez, C.; Cortés, J. Impact of Upwelling Events on the Sea Water Carbonate Chemistry and Dissolved Oxygen Concentration in the Gulf of Papagayo (Culebra Bay), Costa Rica: Implications for Coral Reefs. RBT 2015, 60, 187, doi:10.15517/rbt.v60i2.20004.
52. Kassambara, A. Ggpubr: "ggplot2" Based Publication Ready Plots 2025.
53. Sánchez-Noguera, C.; Lange, I.D.; Cortés, J.; Jiménez, C.; Wild, C.; Rixen, T. Environmental Conditions and Carbonate Chemistry Variability Influencing Coral Reef Composition along the Pacific Coast of Costa Rica. Front. Mar. Sci. 2025, 12, 1606253, doi:10.3389/fmars.2025.1606253.
54. Sánchez-Noguera, C.; Stuhldreier, I.; Cortés, J.; Jiménez, C.; Morales, Á.; Wild, C.; Rixen, T. Natural Ocean Acidification at Papagayo Upwelling System (North Pacific Costa Rica): Implications for Reef Development. Biogeosciences 2018, 15, 2349–2360, doi:10.5194/bg-15-2349-2018.
55. Jiménez, C. Seawater Temperature Measured at the Surface and at Two Depths (7 and 12 m) in One Coral Reef at Culebra Bay, Gulf of Papagayo, Costa Rica. Rev Biol Trop 2001, 49 Suppl 2, 153–161.
56. Montiel-Mora, J.R.; Gómez-Ramirez, E. Calidad fisicoquímica y microbiológica del agua costera en Nicoya, Costa Rica: comparación de tres playas con diferente impacto turístico y administración. URJ 2023, 15, e4763, doi:10.22458/urj.v15i2.4763.
57. Saravia-Arguedas, A.Y.; Vega-Bolaños, H.; Vargas-Hernández, J.M.; Suárez-Serrano, A.; Sierra-Sierra, L.; Tisseaux-Navarro, A.; Cambronero-Solano, S.; Lugioyo-Gallardo, G.M. Surface-Water Quality of the Gulf of Papagayo, North Pacific, Costa Rica. Water 2021, 13, 2324, doi:10.3390/w13172324.

 doi:10.20944/preprints202605.1556.v1

58. Stuhldreier, I.; Sánchez-Noguera, C.; Rixen, T.; Cortés, J.; Morales, A.; Wild, C. Effects of Seasonal Upwelling on Inorganic and Organic Matter Dynamics in the Water Column of Eastern Pacific Coral Reefs. PLoS One 2015, 10, e0142681, doi:10.1371/journal.pone.0142681.
59. Nelson, D.M.; Tréguer, P.; Brzezinski, M.A.; Leynaert, A.; Quéguiner, B. Production and Dissolution of Biogenic Silica in the Ocean: Revised Global Estimates, Comparison with Regional Data and Relationship to Biogenic Sedimentation. Global Biogeochemical Cycles 1995, 9, 359–372, doi:10.1029/95GB01070.
60. Loza Álvarez, S.; Benavides-Morera, R.; Brenes-Rodriguez, C.L.; Ballestero Saxon, D. Estructura Del Fitoplancton En Las Épocas Seca y Lluviosa En El Golfo de Papagayo, Costa Rica. Rev. Mar. Cost. 2018, 10, 9, doi:10.15359/revmar.10-2.1.
61. Shumway, C.A.; Hofmann, H.A.; Dobberfuhl, A.P. Quantifying Habitat Complexity in Aquatic Ecosystems. Freshwater Biology 2007, 52, 1065–1076, doi:10.1111/j.1365-2427.2007.01754.x.
62. McCormick, M. Comparison of Field Methods for Measuring Surface Topography and Their Associations with a Tropical Reef Fish Assemblage. Mar. Ecol. Prog. Ser. 1994, 112, 87–96, doi:10.3354/meps112087.
63. Denis, V.; Ribas-Deulofeu, L.; Sturaro, N.; Kuo, C.-Y.; Chen, C.A. A Functional Approach to the Structural Complexity of Coral Assemblages Based on Colony Morphological Features. Sci Rep 2017, 7, 9849, doi:10.1038/s41598-017-10334-w.
64. Barrera-Falcón, E.; Rioja-Nieto, R.; Hernández-Landa, R.C. Multiscale Structural Complexity Assessment of Coral Reefs Using Underwater Photogrammetry. PLoS One 2025, 20, e0318404, doi:10.1371/journal.pone.0318404.
65. Agudo-Adriani, E.A.; Cappelletto, J.; Cavada-Blanco, F.; Cróquer, A. Structural Complexity and Benthic Cover Explain Reef-Scale Variability of Fish Assemblages in Los Roques National Park, Venezuela. Front. Mar. Sci. 2019, 6, 690, doi:10.3389/fmars.2019.00690.
66. Clements, C.S.; Burns, A.S.; Stewart, F.J.; Hay, M.E. Seaweed-Coral Competition in the Field: Effects on Coral Growth, Photosynthesis and Microbiomes Require Direct Contact. Proc. R. Soc. B. 2020, 287, 20200366, doi:10.1098/rspb.2020.0366.
67. Jompa, J.; McCook, L.J. Effects of Competition and Herbivory on Interactions between a Hard Coral and a Brown Alga. Journal of Experimental Marine Biology and Ecology 2002, 271, 25–39, doi:10.1016/S0022-0981(02)00040-0.
68. Kuffner, I.; Walters, L.; Becerro, M.; Paul, V.; Ritson-Williams, R.; Beach, K. Inhibition of Coral Recruitment by Macroalgae and Cyanobacteria. Mar. Ecol. Prog. Ser. 2006, 323, 107–117, doi:10.3354/meps323107.
69. Burgo, M.; Fabricius, K.E.; Hoey, A.S. The Structure and Composition of Macroalgal Communities Influence Coral Recruitment on an Inshore Reef of the Great Barrier Reef. Coral Reefs 2025, 44, 1315–1326, doi:10.1007/s00338-025-02691-0.
70. Roth, F.; Stuhldreier, I.; Sánchez-Noguera, C.; Morales-Ramírez, Á.; Wild, C. Effects of Simulated Overfishing on the Succession of Benthic Algae and Invertebrates in an Upwelling-Influenced Coral Reef of Pacific Costa Rica. Journal of Experimental Marine Biology and Ecology 2015, 468, 55–66, doi:10.1016/j.jembe.2015.03.018.
71. Alvarado, J.J.; Cortés, J.; Guzman, H.; Reyes-Bonilla, H. Bioerosion by the Sea Urchin Diadema Mexicanum along Eastern Tropical Pacific Coral Reefs. Marine Ecology 2016, 37, 1088–1102, doi:10.1111/maec.12372.
72. Sangil, C.; Sansón, M.; Díaz-Villa, T.; Hernández, J.C.; Clemente, S.; Afonso-Carrillo, J. Spatial Variability, Structure and Composition of Crustose Algal Communities in Diadema Africanum Barrens. Helgol Mar Res 2014, 68, 451–464, doi:10.1007/s10152-014-0401-8.
73. Steneck, R.S. THE ECOLOGY OF CORALLINE ALGAL CRUSTS: Convergent Patterns and Adaptative Strategies. Annu. Rev. Ecol. Syst. 1986, 17, 273–303, doi:10.1146/annurev.es.17.110186.001421.
74. Research and Discoveries: The Revolution of Science through Scuba; Lang, M.A., Marinelli, R.L., Roberts, S.J., Taylor, P.R., Eds.; Smithsonian Contributions to the Marine Sciences; Smithsonian Institution Scholarly Press: Washington, D.C., 2013; Vol. 39;.
75. Harrington, L.; Fabricius, K.; De'ath, G.; Negri, A. RECOGNITION AND SELECTION OF SETTLEMENT SUBSTRATA DETERMINE POST-SETTLEMENT SURVIVAL IN CORALS. Ecology 2004, 85, 3428–3437, doi:10.1890/04-0298.

 doi:10.20944/preprints202605.1556.v1

76. Tebben, J.; Motti, C.A.; Siboni, N.; Tapiolas, D.M.; Negri, A.P.; Schupp, P.J.; Kitamura, M.; Hatta, M.; Steinberg, P.D.; Harder, T. Chemical Mediation of Coral Larval Settlement by Crustose Coralline Algae. Sci Rep 2015, 5, 10803, doi:10.1038/srep10803.
77. Jiménez, C. Arrecifes y ambientes coralinos de Bahía Culebra, Pacífico de Costa Rica: aspectos biológicos, económico-recreativos y de manejo. REVISTA DE BIOLOGIA TROPICAL 2001.
78. Jiménez, C.; Bassey, G.; Segura, Á.; Cortés, J. CHARACTERIZATION OF THE CORAL COMMUNITIES AND REEFS OF TWO PREVIOUSLY UNDESCRIBED LOCATIONS IN THE UPWELLING REGION OF GULF OF PAPAGAYO (COSTA RICA). Rev. Mar. Cost. 2010, 2, 95, doi:10.15359/revmar.2.8.
79. Cortés, J. Latin American Coral Reefs; Elsevier: Amsterdam London, 2003; ISBN 978-0-444-51388-5.
80. Alvarado, J.; Cortés, J.; Fernández, C.; Nivia, J. Coral Communities and Reefs of Ballena Marine National Park, Pacific Coast of Costa Rica. Cienc. Mar. 2005, 31, 641–651, doi:10.7773/cm.v31i4.1140.
81. Glynn, P.W.; Ault, J.S. A Biogeographic Analysis and Review of the Far Eastern Pacific Coral Reef Region. Coral Reefs 2000, 19, 1–23, doi:10.1007/s003380050220.
82. Castrillón-Cifuentes, A.L.; Zapata, F.A.; Wild, C. Physiological Responses of Pocillopora Corals to Upwelling Events in the Eastern Tropical Pacific. Front. Mar. Sci. 2023, 10, 1212717, doi:10.3389/fmars.2023.1212717.
83. Glynn, P.W.; Colley, S.B.; Maté, J.L.; Baums, I.B.; Feingold, J.S.; Cortés, J.; Guzmán, H.M.; Afflerbach, J.C.; Brandtneris, V.W.; Ault, J.S. Reef Coral Reproduction in the Equatorial Eastern Pacific: Costa Rica, Panamá, and the Galápagos Islands (Ecuador). VII. Siderastreidae, Psammocora Stellata and Psammocora Profundacella. Mar Biol 2012, 159, 1917–1932, doi:10.1007/s00227-012-1979-5.
84. Jiménez, C.; Cortés, J. GROWTH OF SEVEN SPECIES OF SCLERACTINIAN CORALS IN AN UPWELLING ENVIRONMENT OF THE EASTERN PACIFIC (GOLFO DE PAPAGAYO, COSTA RICA). BULLETIN OF MARINE SCIENCE 2003, 72.
85. Manzello, D.P. Ocean Acidification Hotspots: Spatiotemporal Dynamics of the Seawater CO2 System of Eastern Pacific Coral Reefs. Limnology & Oceanography 2010, 55, 239–248, doi:10.4319/lo.2010.55.1.0239.
86. Loya, Y.; Sakai, K.; Yamazato, K.; Nakano, Y.; Sambali, H.; Van Woesik, R. Coral Bleaching: The Winners and the Losers. Ecology Letters 2001, 4, 122–131, doi:10.1046/j.1461-0248.2001.00203.x.
87. Nakamura, T.; Van Woesik, R. Water-Flow Rates and Passive Diffusion Partially Explain Differential Survival of Corals during the 1998 Bleaching Event. Mar. Ecol. Prog. Ser. 2001, 212, 301–304, doi:10.3354/meps212301.
88. Gates, R.D.; Edmunds, P.J. The Physiological Mechanisms of Acclimatization in Tropical Reef Corals. Am Zool 1999, 39, 30–43, doi:10.1093/icb/39.1.30.
89. Palacio-Castro, A.M.; Smith, T.B.; Brandtneris, V.; Snyder, G.A.; Van Hooidonk, R.; Maté, J.L.; Manzello, D.; Glynn, P.W.; Fong, P.; Baker, A.C. Increased Dominance of Heat-Tolerant Symbionts Creates Resilient Coral Reefs in near-Term Ocean Warming. Proc. Natl. Acad. Sci. U.S.A. 2023, 120, e2202388120, doi:10.1073/pnas.2202388120.
90. Klepac, C.N.; Barshis, D.J. Reduced Thermal Tolerance of Massive Coral Species in a Highly Variable Environment. Proc. R. Soc. B. 2020, 287, 20201379, doi:10.1098/rspb.2020.1379.
91. Manzello, D.P.; Enochs, I.C.; Bruckner, A.; Renaud, P.G.; Kolodziej, G.; Budd, D.A.; Carlton, R.; Glynn, P.W. Galápagos Coral Reef Persistence after ENSO Warming across an Acidification Gradient. Geophysical Research Letters 2014, 41, 9001–9008, doi:10.1002/2014GL062501.
92. Gorbunov, M.Y.; Kolber, Z.S.; Lesser, M.P.; Falkowski, P.G. Photosynthesis and Photoprotection in Symbiotic Corals. Limnology & Oceanography 2001, 46, 75–85, doi:10.4319/lo.2001.46.1.0075.
93. Kolber, Z.S.; Prášil, O.; Falkowski, P.G. Measurements of Variable Chlorophyll Fluorescence Using Fast Repetition Rate Techniques: Defining Methodology and Experimental Protocols. Biochimica et Biophysica Acta (BBA) - Bioenergetics 1998, 1367, 88–106, doi:10.1016/S0005-2728(98)00135-2.
94. Warner, M.E.; Fitt, W.K.; Schmidt, G.W. Damage to Photosystem II in Symbiotic Dinoflagellates: A Determinant of Coral Bleaching. Proc. Natl. Acad. Sci. U.S.A. 1999, 96, 8007–8012, doi:10.1073/pnas.96.14.8007.

 doi:10.20944/preprints202605.1556.v1

95. Johnson, M.D.; Fox, M.D.; Kelly, E.L.A.; Zgliczynski, B.J.; Sandin, S.A.; Smith, J.E. Ecophysiology of Coral Reef Primary Producers across an Upwelling Gradient in the Tropical Central Pacific. PLoS One 2020, 15, e0228448, doi:10.1371/journal.pone.0228448.
96. Anthony, K.; Hoegh-Guldberg, O. Kinetics of Photoacclimation in Corals. Oecologia 2003, 134, 23–31, doi:10.1007/s00442-002-1095-1.
97. Jassby, A.D.; Platt, T. Mathematical Formulation of the Relationship between Photosynthesis and Light for Phytoplankton. Limnology & Oceanography 1976, 21, 540–547, doi:10.4319/lo.1976.21.4.0540.
98. Falkowski, P.G.; Raven, J.A. Aquatic Photosynthesis; Blackwell science: Malden (Mass.), 1997; ISBN 978-0-86542-387-9.
99. Gorbunov, M.Y.; Falkowski, P.G. Using Chlorophyll Fluorescence to Determine the Fate of Photons Absorbed by Phytoplankton in the World's Oceans. Annu. Rev. Mar. Sci. 2022, 14, 213–238, doi:10.1146/annurev-marine-032621-122346.
100. Jurriaans, S.; Hoogenboom, M. Seasonal Acclimation of Thermal Performance in Two Species of Reef-Building Corals. Mar. Ecol. Prog. Ser. 2020, 635, 55–70, doi:10.3354/meps13203.
101. Alvarado, J.J.; Quesada-Perez, F.; Solano, M.J.; Calvo-Fong, M.; Mena, S. Impact of the 2023–2024 ENSO Event of the North Pacific Coral Reefs of Costa Rica. Diversity 2025, 17, 791, doi:10.3390/d17110791.